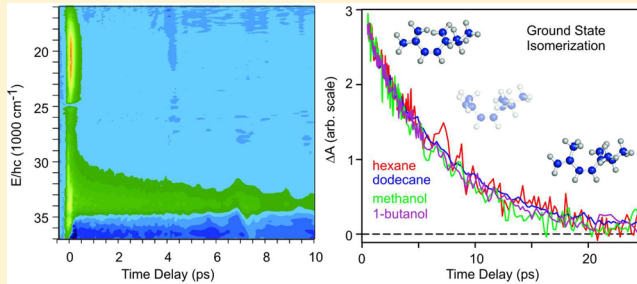


Photochemical Ring-Opening and Ground State Relaxation in α -Terpinene with Comparison to Provitamin D₃

Brenden C. Arruda, Jian Peng, Broc Smith, Kenneth G. Spears, and Roseanne J. Sension*

Department of Chemistry and Department of Physics, University of Michigan, Ann Arbor, Michigan 48109, United States

ABSTRACT: Ultrafast broadband UV-visible transient absorption spectroscopy is used to characterize the photochemistry of α -terpinene, a 1,4-disubstituted-1,3-cyclohexadiene natural product. These results are compared with experiments probing the analogous ring-opening reaction of 7-dehydrocholesterol (DHC, provitamin D₃) and the subsequent relaxation of provitamin D₃. The major experimental results are as follows: (1) Like DHC, but unlike 1,3-cyclohexadiene, α -terpinene exhibits a broad excited state absorption (ESA) spectrum in the visible. The lifetime of the excited state is ca. 0.16 ps in 1-butanol and 0.12 ps in hexane. (2) The state responsible for the ESA is the initially excited state. Fluorescence from this state has a quantum yield of $\sim 2 \times 10^{-5}$. The fluorescence quantum yield is an order of magnitude smaller, and the excited state lifetime is an order of magnitude shorter than that observed for DHC. (3) The initial gZg-triene photoproduct absorbs to the red, and the relaxed tZg-triene product absorbs to the blue of α -terpinene. The gZg \rightarrow tZg reaction of the vibrationally hot photoproduct requires ca. 6.5 ps with no significant dependence on solvent polarity or viscosity. Thermalization occurs on a time scale of 2–4 ps depending on solvent, but shows no particular trends within the solvent series. (4) The conformational relaxation of provitamin D₃ occurs on a similar time scale of ca. 5–8 ps with a modest dependence on the solvent viscosity.



INTRODUCTION

The 1,3-cyclohexadiene (CHD) molecule is the simplest chromophore in a class of cyclic conjugated dienes that undergo a one-quantum photoreaction to form a cis-Z-cis (cZc) hexatriene photoproduct (1,3,5-hexatriene, or HT), where cis refers to the orientation of groups about the single bonds, and Z refers to the orientation about the central double bond (Figure 1). This electrocyclic ring-opening reaction occurs in a $\sigma^2 + \pi^4$ conrotatory fashion according to the Woodward–Hoffmann rules.^{1,2} Due to their efficacy as model photoswitchable molecules, coherent control candidates, and their use as probes of solute–solvent interactions, CHD and HT have been the focus of many steady state and ultrafast spectroscopic experiments^{3–10} as well as high-level calculations.^{11–14} In addition, the CHD backbone is the photoactive chromophore in the biological synthesis of provitamin D₃ (Pre) and vitamin D₃ from 7-dehydrocholesterol (provitamin D₃, Pro, DHC).^{15–18}

Recent nonadiabatic molecular dynamics simulations by Tapavicza et al. explored both the excited state dynamics of CHD and DHC and the ground state conformational relaxation of Pre.¹² Low-temperature excited state simulations indicate that DHC and CHD undergo an initial rapid ca. 10 fs decrease in the length of the C6–C1 and C4–C5 single bonds, accompanied by an increase in the length of the C1=C2 and C3=C4 double bonds and decrease in the length of the C2–C3 single bond. The C–C bond lengths exhibit a very small oscillation in CHD and then relax monotonically to a structure with five equivalent bonds. In DHC, the adjacent rings hinder

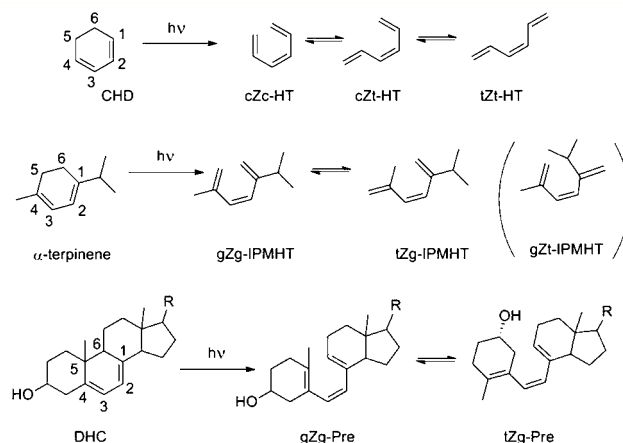


Figure 1. Photochemical ring-opening reactions of CHD, α -terpinene, and DHC (provitamin D₃). The ring-numbering given in the figure, standard for CHD, is used for simplicity in the discussion of the ring-opening reaction for all compounds.

the ring-opening reaction and a damped oscillation of the C–C bond lengths is observed for more than 300 fs. The length of the C5–C6 bond cleaved in the ring-opening reaction increases

Special Issue: Paul F. Barbara Memorial Issue

Received: August 23, 2012

Revised: December 18, 2012

Published: February 6, 2013

monotonically for CHD from 0 to 200 fs, while an induction period of ca. 175 fs with only a slight increase in the bond length followed by a monotonic increase from 175 to 370 fs is observed for DHC. The steric influence of the adjacent rings also influences the conformational relaxation process from the initial all-cis photoproduct to the equilibrium rotamer distribution.

We here focus on a small molecule model for the dynamics of previtamin D₃ formation to explore the influence of substitution on the ground and excited state relaxation involved in CHD ring-opening reactions. The cyclic monoterpene α -terpinene was selected for the initial study because of its small size, which will allow for less computationally demanding modeling, and its substitution geometry which isolates the influence of C1, C4 substitution on the excited state dynamics. In addition, the ground state steric interactions prevent formation of the trans-Z-trans (tZt) conformer, which is also inaccessible in Pre. α -Terpinene is readily available as a natural product used in the food and cosmetics industries.

In a recent matrix isolation study, Marzec et al. used infrared spectroscopy combined with density functional calculations to show that upon UV irradiation α -terpinene undergoes an electrocyclic ring-opening reaction analogous to CHD and DHC, forming the hexatriene product (Z)-2-isopropyl-5-methyl-1,3,5-hexatriene (IPMHT; see Figure 1).¹⁹ As the orientations around the single bonds in the "cis" configurations are helical with a significant distortion from planarity, it is common to refer to this configuration as gauche or gZg. This nomenclature is adopted for the substituted trienes studied here. Because of the variability in the orientation of the methyl and isopropyl groups, the gZg-IPMHT, tZg-IPMHT, and gZt-IPMHT conformers in Figure 1 each represent several different configurations. Marzec et al. include an analysis of all of these configurations in their calculations and in simulated IR spectra.¹⁹ The equilibrium distribution of the α -terpinene photoproduct IPMHT consists predominantly of the tZg conformer. Similarly, the dominant conformer of Pre at equilibrium is the equivalent tZg conformer.¹²

In this paper we report a study of the excited state dynamics of α -terpinene and compare these with the ring-opening reaction in DHC. We also investigate the ground state relaxation dynamics of gZg-Pre and the gZg-IPMHT photoproduct of α -terpinene using ultrafast broadband UV transient absorption spectroscopy. The transient absorption spectra are compared to quantum chemical calculations in an effort to better understand the absorption features. The relaxation dynamics were measured in both alcohols and alkanes spanning a range of viscosities. This is the first such experiment conducted on α -terpinene in solution with ultrafast time resolution.

■ EXPERIMENTAL SECTION

A home-built Ti:Sapphire oscillator and amplifier system was used to produce a 1 kHz pulse train of amplified 800 nm pulses (30 nm fwhm) that was split into a pump and probe arm with 70 mW and 40 mW of power, respectively. The pump arm was frequency tripled to 266 nm using β -barium borate (BBO) crystals. The peak pump pulse energy was approximately 250 nJ at the sample. A broad band UV-visible continuum probe spanning the range from 270 to 600 nm was generated by frequency doubling the 800 nm pulses in the probe arm in BBO and gently focusing the 400 nm second harmonic into a translating CaF₂ window at fixed orientation. The time delay

between the 266 nm pump and the continuum probe was controlled with a mechanical delay stage on the probe arm. The pump and probe pulses were overlapped in the sample, and the probe was then coupled into a spectrometer (Avantes Avaspec-208-USB2-UA). A mechanical chopper was used to modulate the pump pulses (three on, three off), and continuum spectra obtained with pump on and pump off were used to calculate the difference spectra. For measurements confined to the UV region, a low pass filter was placed in the probe beam after the sample to allow only a wavelength range of 270–400 nm into the spectrometer. This provided a better dynamic range in the UV measurement by eliminating the stronger visible continuum. The polarization of the pump and probe beams were oriented at magic angle (54.7°) with respect to each other to eliminate contributions to the dynamics arising from dipole reorientation.

A 1 mm path length quartz flow cell was used to contain the sample and eliminate build-up of photoproduct in the focus of the beams. The instrument response function in the UV region ($\lambda < 390$ nm) ranged from 150 to 300 fs, as determined by the full-width at half-maximum (fwhm) for the coherent two-photon absorption peak observed in the solvent when the pump and probe pulses overlap. This was sufficient to measure the ground state dynamics of IPMHT and Pre, which occur on a 1–10 ps time scale. As the excited state lifetime of α -terpinene is on the order of 100–160 fs, special care was taken to optimize the pulse duration to less than 100 fs for measurements of the excited state absorption (ESA) in the visible. For all measurements the chirp on the continuum probe was corrected by fitting the coherent spike to a third-order polynomial and ensuring that the peak of the spike was at t_0 across the whole spectrum.

With UV excitation pulses multiphoton absorption and ionization of the solvent is always a potential complication that must be taken into account. In the experiments reported here care was taken to ensure that the solvent contribution was small by limiting the excitation pulse to ca. 250 nJ and by measuring the solvent-only transient absorption spectrum following each sample measurement. In the data analysis the residual solvent signal was subtracted from the sample signal. The wavelength range $\lambda = 340$ –400 nm at time delays greater than 10 ps where only the solvent contributed to the sample signal was used to scale the solvent contribution. The scale factor was always less than 1 due to attenuation of the pump by the sample and was generally 0.5–0.8.

Steady state photolysis experiments were conducted using the unfiltered output of a mercury arc lamp (7A, 125 V power supply) and a Shimadzu UV-2401pc UV-vis spectrometer with a wavelength range of 190 to 1100 nm and a resolution of 0.1 nm. Photolysis measurements were done in heptane and methanol. The photolysis of DHC in methanol required careful deoxygenation to avoid secondary product formation. Fluorescence measurements were performed using a Jasco FP-6500 spectrofluorometer at a concentration of 0.5 mM. DHC (98%), α -terpinene (95%), and all solvents were acquired from Sigma-Aldrich and used without further purification. All solutions for transient absorption experiments were made at approximately 1 mM.

Optimized structures and single point energies were calculated using a time-dependent density functional theory (TD-DFT) approach in the Gaussian03 software package.²⁰ All calculations employed the 6-311++G(d,p) basis set and the B3LYP density functional. The transition state optimizations

were conducted using the Synchronous Transit-Guided Quasi-Newton (STQNI) method.²¹ The correct transition state was verified using the results of frequency calculations to ensure that only one imaginary (negative) frequency corresponding to the reactive coordinate was present.

RESULTS

Steady State Photolysis and Fluorescence of α -Terpinene. The steady state absorption spectra of α -terpinene and its photoproducts at various UV irradiation times are shown in Figure 2. α -Terpinene exhibits a broad absorption

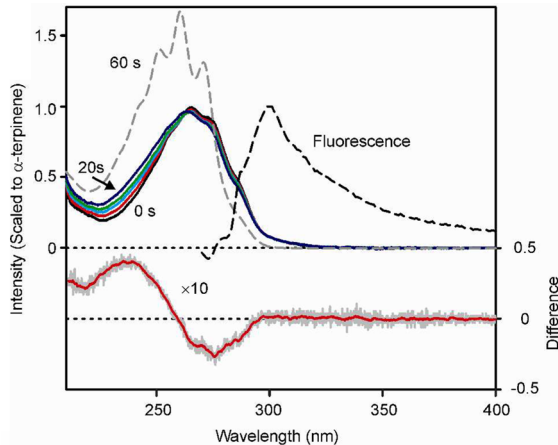


Figure 2. Steady state absorption spectra of α -terpinene and its photoproducts at various UV irradiation times (solid black: α -terpinene absorption spectrum; dashed black: α -terpinene fluorescence; red: 5 s; light blue: 10 s; green: 15 s; dark blue: 20 s; dashed gray: 60 s). The difference curve is between α -terpinene and the 5 s photoproduct. This spectrum has been offset and multiplied by 10 for clarity. The gray line is the raw data, while the red line has been smoothed with a 2 nm running average. This difference spectrum is consistent with the long-time difference spectrum in the ultrafast measurements.

band centered at 265.5 nm with a slight shoulder around 286 nm. From the absorption measurements the extinction coefficient at peak wavelength for α -terpinene is estimated to be $6620 \pm 40 \text{ M}^{-1} \text{ cm}^{-1}$. The evolution of the spectrum with UV irradiation is consistent with conversion of α -terpinene to the Z-type photoproduct at the shortest irradiation times. Longer irradiation times lead to reabsorption and the growth of an E-type isomer spectrum. This growth is gradual, and the assignment to a new photoproduct is evidenced by a shift in the zero-crossing point in the difference spectrum from 259 to 275 nm. The spectrum for the E isomer is blue-shifted from α -terpinene and shows a distinct vibronic structure with three identifiable bands at 270.5 nm, 260.5 nm, and 251.5 nm. The vibronic structure is characteristic of planar hexatrienes. The steady state spectra of both α -terpinene and its photoproducts are virtually identical in all solvents under investigation here.

Time integrated fluorescence measurements on α -terpinene in heptane show a fluorescence spectrum peaking at 300 nm. By comparison with the well-characterized fluorescence of *trans*-stilbene, an estimate of the excited state lifetime of α -terpinene can be made. The fluorescence quantum yield for *trans*-stilbene in heptane is estimated to be slightly higher than the quantum yield in hexane (4.33×10^{-2} at 299.8 K^{22}). The quantum yield in heptane is estimated as 5.0×10^{-2} .^{18,23} Using

this value as a standard, the fluorescence quantum yield for α -terpinene is estimated as $\phi_f = \sim 2 \times 10^{-5}$. The Strickler–Berg equation²⁴ can be used to estimate the radiative lifetime of α -terpinene in heptane solution with the approximation $n = n_D$:

$$k_r \cong \frac{8\pi n^2 2303}{N_a c^2} \langle \nu_f^3 \rangle \int \frac{\epsilon(\nu_a)}{\nu_a} d\nu_a \quad (1)$$

Using the Strickler–Berg equation, the radiative lifetime of α -terpinene is estimated to be on the order of 6 ns. Given both the fluorescence quantum yield and the radiative lifetime, the fluorescence lifetime of the excited state can be estimated as $(2 \times 10^{-5})(6 \times 10^6 \text{ fs}) = \sim 120 \text{ fs} (\pm 100 \text{ fs})$.

Transient Absorption Spectroscopy of α -Terpinene.

Time-resolved transient absorption spectra (TA spectra) were obtained for α -terpinene in seven solvents chosen to cover a wide range of solvent polarities and viscosities. All spectra show a spike at $t = 0 \text{ ps}$ corresponding to a two-photon absorption of the solvent and solute when there is maximum temporal overlap of the pump and probe pulses. Solvent scans yielded only minimal dynamics beyond this spike, which provides the cross-correlation of the pump and probe pulses. The solvent signal was subtracted from all of the α -terpinene spectra before analysis.

The early time UV–visible transient absorption spectra of α -terpinene in hexane, 1-propanol, and 1-butanol are plotted in Figure 3. The spectrum in 1-butanol was obtained with a continuum generated by focusing 800 nm in CaF_2 and the spectra in hexane and 1-propanol were obtained with a continuum generated by focusing 400 nm in CaF_2 . At early times, the spectra in the alcohols are characterized by a strong

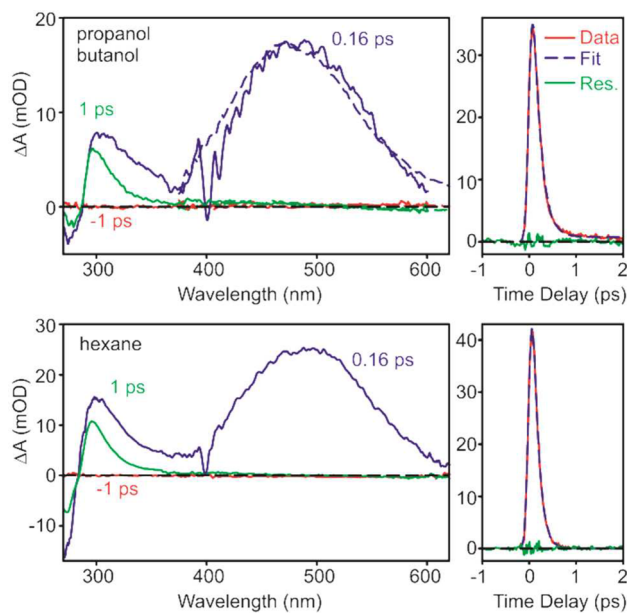


Figure 3. ESA of α -terpinene in 1-propanol (solid line), 1-butanol (dashed line), and *n*-hexane. The solvent-only signal has been subtracted from the solvent + solute scans. The dip at ca. 400 nm is an artifact of residual 400 nm used to produce the continuum probe. There is a broad visible absorption band peaking at ca. 470 nm in the alcohols and 480 nm in hexane. The decay of the ESA between 470 and 475 nm in 1-butanol is plotted in the top right panel. The decay in hexane is plotted in the lower right panel. A fit to an exponential decay of the absorption yields an excited state lifetime of 0.16 ps in 1-butanol and 0.12 ps in *n*-hexane.

peak in the visible region with a maximum at ca. 470 nm. This absorption is similar to the visible absorption band observed following excitation of DHC. By contrast, no ESA is observed in the visible region following excitation of CHD. The ESA of α -terpinene decays with a lifetime of 0.16 ps in 1-butanol. In hexane the ESA is red-shifted slightly, with the maximum at ~480 nm, and decays with a lifetime of 0.12 ps. The decay of the ESA is consistent with the fluorescence lifetime deduced from the quantum yield above and likely reflects decay of the state initially populated following excitation at 266 nm.

The UV absorption band observed in the TA spectrum decays on a much longer time scale. Difference spectra obtained following excitation of α -terpinene in hexane at 266 nm are shown in Figure 4 for time delays of 0.5–100 ps and probe

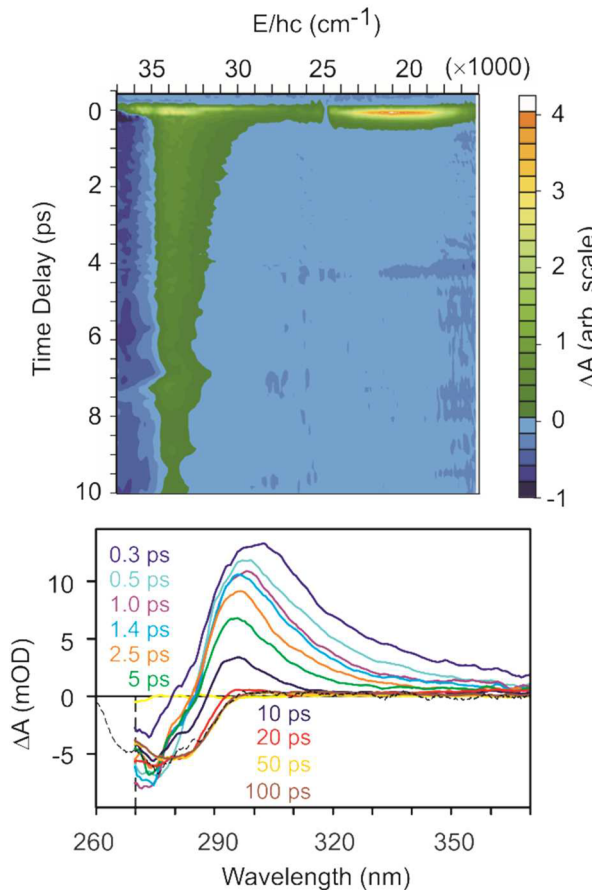


Figure 4. Top: Transient absorption spectra of α -terpinene in hexane at various time delays. The main spectral features are a bleach on the blue edge and a peak at 300 nm. The peak appears at early times and decays with a time constant around 6 ps in all solvents. No significant change in peak shapes is observed between the different solvents.

wavelengths between 270 and 370 nm. A negative signal corresponding to the ground state bleach of α -terpinene is seen at 270–280 nm. This bleach is present for all time delays following the initial instrument limited spike corresponding to two-photon absorption of the solvent and/or solute. A positive absorption peak is observed ranging from approximately 285 to 330 nm. TA spectra in all solvents studied here, hexane, decane, dodecane, hexadecane, cyclohexane, methanol, 1-propanol, and 1-butanol, behave similarly with little difference in the nature of the spectral or kinetic components.

Kinetic traces of α -terpinene in dodecane at various wavelengths are shown in Figure 5. These traces were analyzed

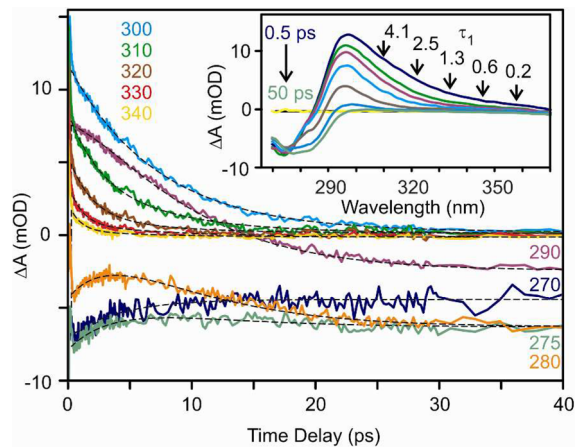


Figure 5. Kinetic traces (colored) and fits (black) of α -terpinene in dodecane at representative wavelengths indicated on the plot. The fits have residuals centered at 0 with no features other than noise. The inset shows the wavelength dependence of the fast component in the biexponential fit. The rate becomes faster (time constant becomes smaller) on the red edge of the absorption. The spectra are plotted for time delays of 0.5, 1.4, 2.5, 5, 10, 20, and 50 ps.

using a multiexponential fitting routine in a global analysis program. A multiexponential model was used because it captures the dynamics at all wavelengths while avoiding overinterpretation of the spectrum. Two exponentials are required to fit the data at all wavelengths. A third amplitude is required to account for permanent photoproduct formation. The need for two exponential decay components is most clearly demonstrated by the rise and decay at $\lambda = 280$ nm. Using fewer exponentials in the model led to a nonzero residual, while adding more exponentials did not improve the χ^2 value for the fit to the model. At 300 nm, only one exponential is required to fit the data, 7.1 ps in dodecane. For wavelengths to the red of 300 nm, the additional fitting parameter has a wavelength dependence as illustrated in the inset to Figure 5. By 360 nm, this component is indistinguishable from the decay of the visible ESA. For probe wavelengths between 270 and 300 nm, the second exponential does not vary significantly with wavelength. The time constant of this component is 4.2 ps \pm 0.2 ps in dodecane.

The data in the other alkane and alcohol solvents studied here are similar. The traces are well modeled by a biexponential decay at most wavelengths. The decay of the peak of the positive absorption signal around 300 nm requires only a single exponential ranging from 5.5 to 7.4 ps. The decay constants obtained from the fits are given in Table 1. There is no clear trend with macroscopic solvent properties, including solvent shear viscosity. The data, plotted in Figure 6, are scattered around a central value.

Quantum Chemical Calculations on α -Terpinene. Optimized structures of α -terpinene and the primary rotamers of its photoproducts were used for a set of excited state and ground state calculations. The calculated ground state single point energies, oscillator strengths, and energy differences between the ground and first singlet excited states are summarized in Table 2. The ground state energies are in good agreement with the calculations reported by Marzec et

Table 1. Viscosities and the Time Constants from the Exponential Fits Across the UV Portion of the Spectrum of α -Terpinene

solvent	η (mPa s) ^a	τ_1 (ps) ^b	τ_2 (ps) ^c
hexane	0.300	2.8 ± 0.25^d	6.7 ± 0.25
decane	0.838	3.3 ± 0.25	7.3 ± 0.25
dodecane	1.383	4.2 ± 0.20	7.1 ± 0.20
hexadecane	3.032	1.7 ± 0.25	5.5 ± 0.25
cyclohexane	0.894	3.7 ± 0.50	7.4 ± 0.50
methanol	0.544	3.6 ± 0.35	5.9 ± 0.35
1-propanol	1.945	2.9 ± 0.25	6.0 ± 0.25
1-butanol	2.544	3.8 ± 0.27	6.3 ± 0.27

^aViscosities are reported for 25 °C.²⁵ ^bThe fast component, τ_1 , depends on solvent and wavelength. The values in the table are from the blue portion of the spectrum where τ_1 is constant across wavelength. For wavelengths >320, the rate of the fast component increases with wavelength. ^cThe time constant τ_2 characterizes the decay of the absorption peak at 300 nm. ^dThe error represents the range at which the χ^2 for the fit remains within 0.01 of the best fit.

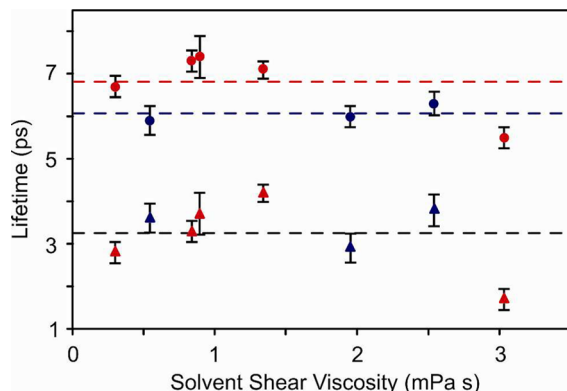


Figure 6. Lifetime of the fast (triangles) and slow (circles) components for the UV absorption following excitation of α -terpinene. The blue symbols are measurements in alcohols, the red symbols are measurements in alkanes.

Table 2. Excited State and Single Point Ground State Energies and Oscillator Strengths

conformer	oscillator strength	singlet transition (nm)	ground state energy (kJ/mol)
α -terpinene	0.2241	277.83	0
gZg-IPMHT	0.1168	282.4	100.4
tZg-IPMHT	0.3835	265.46	94.2
gZt-IPMHT	0.2500	268.74	99.1
tEt-IPMHT	0.8359	270.7	62.2

al.¹⁹ The initial gZg conformation of the photoproduct is predicted to absorb to the red of α -terpinene, while other conformations absorb to the blue of α -terpinene. Vibrational frequency calculations on the gZg and tZg conformations as well as the transition state between the two were performed in order to obtain free energies. These structures and their energies are shown in Figure 7. The Gibb's free energy of activation for the gZg to tZg interconversion is calculated to be 16.5 kJ/mol, while the enthalpy of activation is 9.9 kJ/mol. The calculated Gibb's free energy and the enthalpy of the gZg to tZg reaction are -3.5 and -5.1 kJ/mol, respectively.

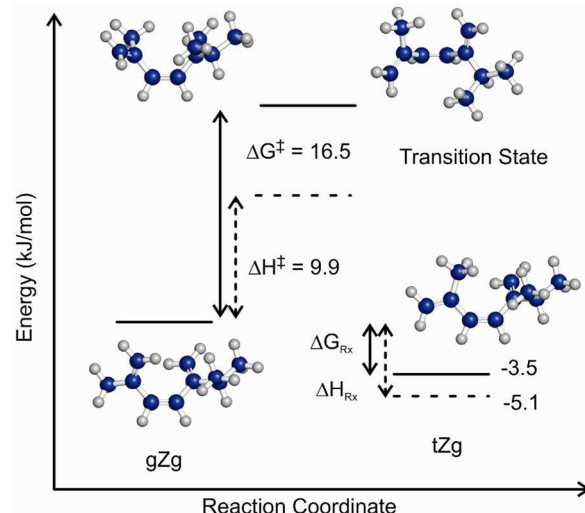


Figure 7. Thermodynamic quantities obtained from frequency calculations in the Gaussian 03 software package using the B3LYP density functional and the 6-311++G(d,p) basis set.^{20,26} The free energy of activation has a large entropic component, and the overall energy decreases as the photoproduct interconverts from gZg to tZg.

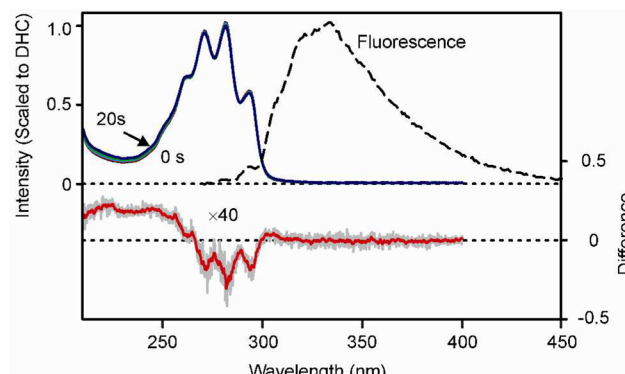


Figure 8. Steady state absorption spectra of DHC and its photoproducts in heptane at various UV irradiation times (solid black: DHC absorption spectrum; dashed black: DHC fluorescence; red: 5 s; light blue: 10 s; green: 15 s; dark blue: 20 s). The difference curve is between DHC and the early time photoproduct observed between 5 and 15 s. This spectrum has been offset and multiplied by 40 for clarity. The gray line is the raw data, while the red line has been smoothed with a 1 nm running average.

Steady-State and Transient Spectroscopy of DHC. The steady state absorption spectra of DHC and its photoproducts at various UV irradiation times as well as the normalized, solvent-subtracted fluorescence spectrum of DHC are shown in Figure 8. The fluorescence spectrum is consistent with that reported earlier.¹⁸ The zero-point crossings in the difference spectra obtained in the photolysis measurements are stable for the first 15 s and then begin to shift as additional photoproducts accumulate. The difference spectrum shown in the lower panel of Figure 8 is a weighted average of the difference at 5 s ($w = 1$), 10 s ($w = 0.45$) and 15 s ($w = 0.32$) scaled to the intensity of the 5 s difference.

For comparison with the results reported above for α -terpinene, UV transient absorption spectra were obtained for DHC in *n*-heptane, dodecane, methanol, and 2-butanol. The UV-visible transient absorption spectrum of DHC in 2-butanol is summarized in Figure 9. The ESA in the visible region is

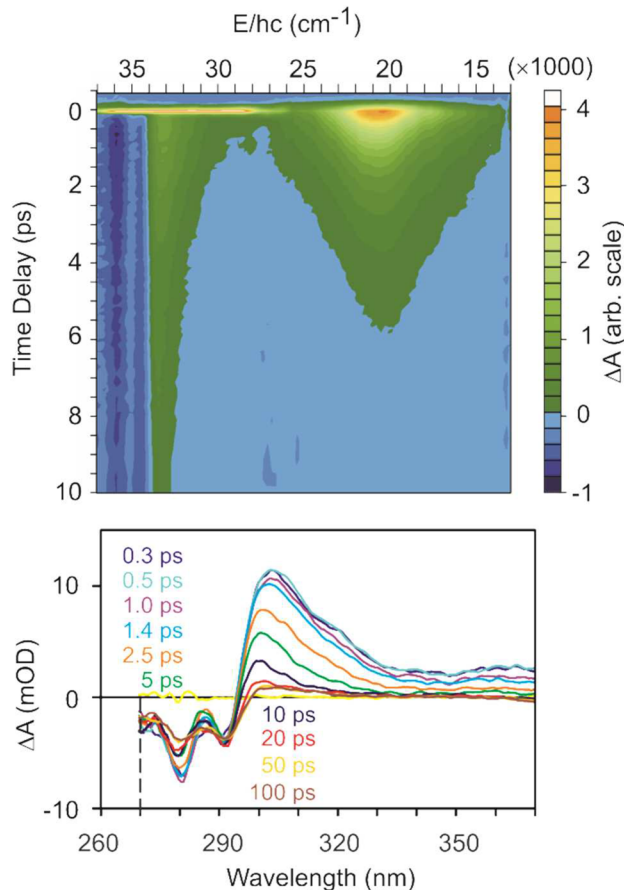


Figure 9. Transient absorption spectra of DHC at various time delays. The contour plot shows both the spectral behavior in the UV region as well as the ESA in the visible. The plots here are for DHC in 2-butanol.

identical to that reported earlier.¹⁸ The time-dependent difference spectra in the ultraviolet region are in reasonably good agreement with previous TA experiments which utilized selected single wavelength probes.^{15–17} The current data sets, however, are more complete and provide a better overall picture of the relaxation dynamics of the previtamin D₃ molecule formed following the excited state ring-opening reaction.

The main features in the UV difference spectra are a net bleaching signal observed between 270 and 295 nm and a broad net absorption peak around 305 nm. A global fitting algorithm was used to analyze the evolution of the difference spectrum. Contrary to the conclusions of earlier single wavelength measurements, the DHC fitting parameters show little wavelength dependence. The data is appropriately fit using two exponential decay components and a constant component representing formation of the long-lived photoproduct. The fast component (~1.1–1.8 ps) is in good agreement with the average decay of the visible absorption and is assigned to the decay of the electronically excited state.^{12,13,15,22} The longer time scale decay ranges from 5 ps in methanol and heptane to 8.5 ps in dodecane and represents the decay of a red-shifted absorption band. The assignment for this absorption will be considered in the discussion below. A summary of the time constants obtained for the four solvents studied here is provided in Table 3.

Table 3. Time Constants Obtained from Global Fits Across a Wavelength Range in DHC of 275–370 nm^a

solvent	η (mPa s)	τ_1 (ps)	τ_2 (ps)
heptane	0.387	1.1 ± 0.45	5.1 ± 0.45
dodecane	1.383	1.4 ± 0.45	8.5 ± 0.45
methanol	0.544	1.5 ± 0.60	5.4 ± 0.60
2-butanol	3.096	1.8 ± 0.25	6.2 ± 0.25

^aViscosities are reported for 25° C.²³

DISCUSSION

Assignment of Transient Absorption Features of α -Terpinene. The qualitative features in the transient absorption spectra of α -terpinene are remarkably similar to the trends observed in DHC. There is a strong ESA assigned to a transition from the initially excited state. The estimated fluorescence lifetime of the initially excited state is in good agreement with the measured lifetime of the visible ESA. The excited state decay in α -terpinene is approximately an order of magnitude faster than that observed for DHC, on the same general time scale as the rapid nonadiabatic decay back to the ground state observed for CHD.^{1,5,9} However, the presence of a fluorescence signal and an ESA suggest that the electronic states involved in the ring-opening of α -terpinene are more similar to those of DHC than CHD.¹⁸ CHD has a fluorescence lifetime of ca. 10 fs,²⁷ and no ESA is observed in the visible region of the spectrum. Control experiments using a dump pulse to control dynamics are also consistent with the hypothesis that population on the optically allowed state persists for no longer than 50 fs.⁹

The solvent dependence of the excited state decay in DHC suggests the presence of both an intrinsic barrier of ca. 2 kJ/mol and a solvent induced barrier influenced by the solvent viscosity.¹⁸ There may be a small solvent dependence in the excited state decay of α -terpinene, but the overall effect is within the errors of the present measurement and would require more precise measurements with better time resolution and as a function of temperature to be fully characterized. In any case, the order of magnitude difference between the lifetime of the excited state in DHC and α -terpinene suggests that the intrinsic and environmental barriers for the excited state are much smaller than $k_B T$ at room temperature for the α -terpinene molecule.

The features observed in the UV region of the difference spectrum obtained following excitation of α -terpinene reflect the vibrational cooling and conformational relaxation of the hexatriene product (IPMHT) formed following the photochemical ring-opening reaction. TD-DFT calculations predict that gZg-IPMHT will have an absorption band with approximately half the intensity and shifted approximately 5 nm to the red of the corresponding transition in α -terpinene. Molecules in a tZg-IPMHT conformation are predicted to absorb 12 nm to the blue, with an oscillator strength about 70% larger than the corresponding transition of α -terpinene. These calculations are in qualitative agreement with the steady state photolysis and ultrafast transient absorption measurements.

Adding a scaled amount of the α -terpinene spectrum to the difference spectrum in the lower panel of Figure 2 allows for a rough estimate of the location and shape of the steady state IPMHT photoproduct spectrum (predominantly tZg-IPMHT). Varying the scale factor sets limits for the relative magnitude and peak shifts of the gZg-IPMHT and tZg-IPMHT spectra. The lower limit is set by the requirement that the estimated tZg

spectrum be positive, while increasing the scale causes the tZg spectrum to approach the initial α -terpinene spectrum. The cartoon spectra shown in Figure 10 represent a reasonable

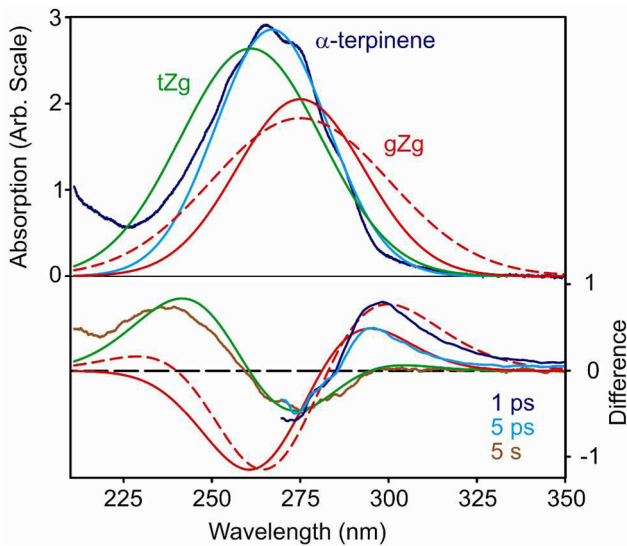


Figure 10. Cartoon spectra based on the calculated spectra for α -terpinene and IPMHT photoproducts. The dark blue spectrum in the top panel is the measured spectrum of α -terpinene. The light blue is a Gaussian fit to the α -terpinene spectrum. The green is an estimated spectrum of tZg-IPMHT. The red lines are estimated spectra of hot (dashed) and cool (solid) gZg-IPMHT. The bottom panel compares the difference spectra at 1 ps, 5 ps, and steady state (see Figure 4) with the difference spectra calculated from the Gaussian spectra plotted in the top panel.

estimate and help elucidate the key features in the transient absorption. We stress, however, that this is a qualitative treatment because the spectra for gZg and tZg-IPMHT are not known independently and likely contain asymmetries not captured by a Gaussian function.

The initial photoproduct is formed in a gZg conformation consistent with the principle of least motion.¹⁹ The peak at ca. 300 nm in the ultrafast transient absorption measurements reflects the formation, thermalization, and conformational relaxation of this initial gZg-IPMHT photoproduct. The red-shift of the gZg-IPMHT spectrum in Figure 10 is ca. 8 nm, and the oscillator strength of this spectrum appears to be comparable to the spectrum of α -terpinene. The picosecond dynamics in the TA spectra represent a combination of spectral narrowing as the molecule cools and population decay as the gZg-IPMHT conformation isomerizes to an equilibrium distribution of conformers dominated by tZg-IPMHT configurations.

The difference spectra obtained with time delays ≥ 50 ps and in the steady state photolysis measurement are characterized by the bleach of the α -terpinene absorption and the appearance of an absorption peak to the blue of α -terpinene. The peak of this absorption falls outside of the spectral window of the ultrafast measurements, but is clearly seen in the steady state spectrum. The estimate plotted in Figure 10 represents a 6 nm blue shift of the tZg spectrum with respect to α -terpinene and an oscillator strength comparable to that of both α -terpinene and the gZg conformer. This is a qualitative analysis, and discrepancies in the magnitude of the peak shifts and peak heights are likely caused by limitations in the ability to extract

the tZg and gZg spectra from the data as well as limitations in the accuracy of the calculations.

As described above, the ultrafast spectral evolution of α -terpinene in solution can be fit well using a linear combination of two exponential terms with amplitude and decay constants as the fitting parameters and constant corresponding to the permanent photoproduct. The ca. 7 ps decay is associated with the depletion of red-absorbing gZg-IPMHT via conformer interconversion to tZg-IPMHT. The faster decay component is characterized by a wavelength-dependent decay of the intensity on the red edge of the spectrum and an increase in the absorption intensity around the peak of the gZg-IPMHT transition. This component likely reflects the approach to thermal equilibrium with the surrounding solvent as the spectrum narrows and conformer interconversion occurs. The comparison of the dashed and solid red lines representing gZg-IPMHT in Figure 10 illustrate the expected influence of spectral narrowing on the time-resolved spectra.

Assignment of decay processes in DHC. The ultrafast excited state and ground state dynamical processes in DHC have been well characterized by a number of experimental studies and high-level calculations.^{12,15–18} Tang et al. used broadband visible transient absorption spectroscopy to demonstrate that the excited state decay is biexponential with time constants of 0.4–0.65 ps and 1.0–1.8 ps depending on solvent and the temperature.¹⁸ The probable explanation for the biexponential decay behavior is a branching down different decay pathways with distinct populations on the excited state surface as the CHD ring opens.^{18,28} Meyer-Ilse et al. performed UV femtosecond time-resolved circular dichroism (TRCD) measurements that provide further support for a fast ring-opening reaction.²⁹ TRCD provides a unique probe for the ring-opening process because it is sensitive to the change in chirality caused by the ring-opening reaction. The results of the TRCD measurements show a chirality change on a time scale of 1–2 ps. This allows for a confident assignment of the picosecond component in the UV TA spectra to the ring-opening process on the electronic excited state.

In Figure 11 we show a comparison of the early (2.5 ps) and late (>100 ps) transient difference spectra of the photoproduct obtained following excitation of DHC in methanol and heptane. These difference spectra are compared with the steady state difference spectrum obtained after 5–10 s of UV photolysis (see Figure 8), the spectrum of DHC and the estimated spectrum of the previtamin D₃ photoproduct. The spectrum of Pre was obtained by adding the DHC spectrum to the 5s difference spectrum until the vibronic structure between 265 and 300 nm was minimized in the photoproduct spectrum. The Gaussian fit to the product spectrum in heptane peaks at ca. 260 nm with a fwhm of ca. 6500 cm⁻¹. In methanol, the Gaussian fit peaks at 265 nm with a fwhm of ca. 6000 cm⁻¹. This is in reasonable agreement with the spectrum reported by Fuss et al. in ethanol.¹⁷

In previous work Anderson et al. assigned the 5–6 ps decay component observed in the UV to vibrational relaxation of the initial gZg-Pre photoproduct on the ground state and a long time decay of 100 ± 20 ps to the conformational isomerization on the ground state, producing an equilibrium mixture of gZg and tZg conformers.¹⁶ However, the 100 ps component was reported to have very low amplitude relative to the other components and is not observed in the data reported here when care is taken to account for and minimize contributions from multiphoton excitation of the solvent. The 5–8 ps

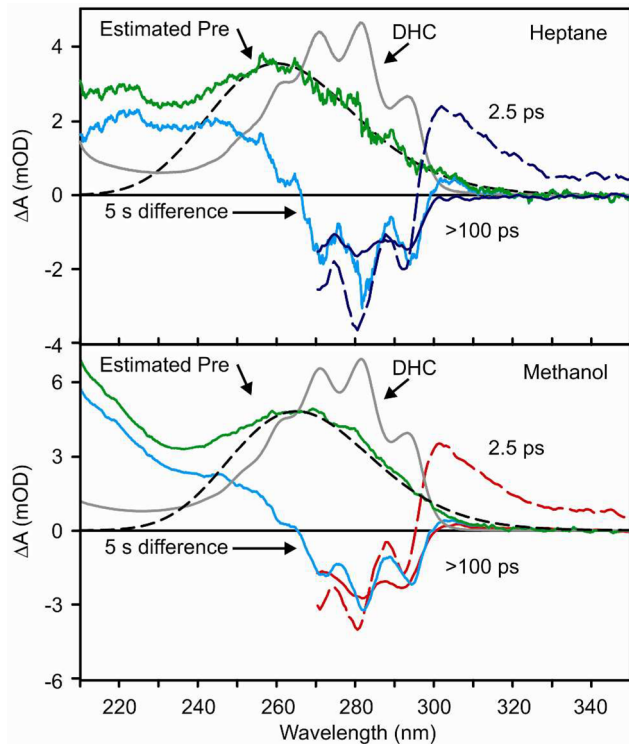


Figure 11. Comparison of the early (dashed, 2.5 ps) and late (solid, >100 ps) difference spectra following photolysis of DHC in methanol (bottom, red) and heptane (top, blue). The steady state spectra of DHC (gray), the early steady state difference spectrum (light blue, see Figure 8), and the estimated spectrum of previtamin D₃ (green) are also shown for each solvent. The black dashed line is a Gaussian fit to the estimated spectrum of previtamin D₃.

component observed in DHC is likely associated, as in α -terpinene, with the decay of the gZg conformer of Pre produced in the initial ring-opening process to a mixture of rotamers approaching that expected at thermal equilibrium. This 5–8 ps decay component in the transient spectrum may also contain a contribution due to vibrational relaxation of both gZg-Pre and DHC following ground state recovery.

Tapavicza et al. used ab initio excited state nonadiabatic dynamics simulations to study DHC photochemistry. They find that, following relaxation to the ground state, Pre adopts the equilibrium distribution of rotamers within ~6 ps.¹² The present experiments are consistent with this simulation and suggest that there is a rapid ground state conformer interconversion from the hot gZg-Pre conformation to the tZg-Pre conformation. The interconversion depends only modestly on the solvent environment, with the relaxation in the more viscous alkane and alcohol solvents only slightly slower than that in the less viscous solvents.

For time scales longer than 50 ps, there is a small residual absorption on the red edge of the DHC spectrum in methanol and 2-butanol. This absorption is not observed in heptane or dodecane where the difference decays to zero on the red edge. The difference spectrum observed for time-delays greater than 50 ps is qualitatively similar to the steady state difference spectrum, but is not as structured (see Figure 11). This may reflect a limitation of the transient measurement, but more likely reflects continued conformational relaxation of Pre on the ground state surface. This complex molecule can adopt a wide

range of similar configurations as Tapavicza et al. observe in their simulations.¹²

We note as well that the distribution formed following the 6 ps relaxation in solution need not be the distribution of gZg-Pre and tZg-Pre expected at thermal equilibrium. Earlier measurements on hexatriene and CHD demonstrated that ca. 5–7% was trapped in the higher energy tZc-HT conformation and underwent thermal relaxation to tZt-HT on a time scale greater than 100 ps.^{3,4} Likewise, single wavelength measurements by Fuss et al. on DHC in ethanol suggest that there is a ca. 100 ps decay component corresponding to thermal interconversion of gZg-Pre \rightarrow tZg-Pre.¹⁷ The temperature dependence of this component yielded an interconversion barrier of 15.5 ± 1 kJ/mol. It is possible that the ca. 100 ps component observed by Fuss et al. represents the final approach to equilibrium of a small excess of excited conformers trapped as the initial hot photoproduct cools through energy transfer to the solvent. The probe wavelengths used in the single wavelength temperature-dependent measurements of Fuss et al. were near the zero-crossing point between 260 and 270 nm, outside the range of the present measurements. In this region, the data will be more sensitive to small changes in the conformational populations than at the longer probe wavelengths used here.

CONCLUSION

The goal of this study was to characterize the photochemistry of α -terpinene and the structural dynamics of the IPMHT photoproduct following the ring-opening reaction. These measurements are compared with analogous experiments probing the photochemistry of provitamin D₃ and the subsequent relaxation of previtamin D₃. Quantum chemical calculations were used to justify the assignment of the absorption features of the gZg-IPMHT and tZg-IPMHT photoproducts in the steady state and ultrafast regimes.

Following UV excitation, both α -terpinene and DHC exhibit visible ESA from the initially excited state. No such absorption is observed for CHD. The ESA decays on a time scale of ~150 fs in α -terpinene and 1–2 ps in DHC.¹⁸ The fluorescence quantum yields and excited state lifetimes are in good agreement, demonstrating that the initially excited state has a lifetime much longer than the corresponding state of CHD. The ring-opening reaction of both α -terpinene and DHC occurs on essentially the same time scale as the decay of the initially excited state.

The initial gZg-IPMHT triene photoproduct absorbs to the red of the α -terpinene ground state spectrum. Ultrafast UV transient absorption measurements show that conformer interconversion from the gZg-IPMHT triene photoproduct to tZg-IPMHT occurs on a 5.5 to 7.4 ps time scale with no systematic dependence on solvent polarity or viscosity. Thermalization occurs on a time scale of 2–4 ps depending on solvent, also with no particular trends within the solvent series. The UV transient spectrum of the gZg-Pre product formed following excitation of DHC is similar to that of gZg-IPMHT. This photoproduct is also characterized by a red-shifted absorption with a peak at ca. 300 nm in the ultrafast difference spectrum. The solvent dependence for the decay of gZg-Pre is somewhat larger than observed for gZg-IPMHT, ranging from 5.1 to 8.5 ps, but still relatively small. The similarity in time scales for gZg-IPMHT and gZg-Pre is surprising given the large size difference in the substitutions around the triene structure. Future studies of these ring-opening reactions and the relaxation of the resulting triene

systems will involve using a shorter wavelength UV probe to characterize the formation of the photoproduct more completely along with molecular dynamics simulations in an attempt to understand the mechanism for the conformational relaxation and the reason for the small influence of solvent environment on the process.

AUTHOR INFORMATION

Notes

The authors declare no competing financial interest.

ACKNOWLEDGMENTS

This work was supported in part by NSF Grants CHE-0718219 and CHE-1150660.

REFERENCES

- (1) Deb, S.; Weber, P. M. *Annu. Rev. Phys. Chem.* **2011**, *62*, 19–39.
- (2) Woodward, R. B.; Hoffmann, R. *Angew. Chem., Int. Ed.* **1969**, *8*, 781–853.
- (3) Anderson, N. A.; Pullen, S. H.; Walker, L. A.; Shiang, J. J.; Sension, R. *J. J. Phys. Chem. A* **1998**, *102*, 10588–10598.
- (4) Harris, D. A.; Orozco, M. B.; Sension, R. *J. J. Phys. Chem. A* **2006**, *110*, 9325–9333.
- (5) Kosma, K.; Trushin, S. A.; Fuss, W.; Schmid, W. E. *Phys. Chem. Chem. Phys.* **2009**, *11*, 172–181.
- (6) White, J. L.; Kim, J.; Petrovic, V. S.; Bucksbaum, P. H. *J. Chem. Phys.* **2012**, *136*, 054303.
- (7) Carroll, E. C.; Pearson, B. J.; Florean, A. C.; Bucksbaum, P. H.; Sension, R. *J. J. Chem. Phys.* **2006**, *124*, 114506.
- (8) Carroll, E. C.; White, J. L.; Florean, A. C.; Bucksbaum, P. H.; Sension, R. *J. J. Phys. Chem. A* **2008**, *112*, 6811–6822.
- (9) Kim, J.; Tao, H. L.; White, J. L.; Petrovic, V. S.; Martinez, T. J.; Bucksbaum, P. H. *J. Phys. Chem. A* **2012**, *116*, 2758–2763.
- (10) Garavelli, M.; Page, C. S.; Celani, P.; Olivucci, M.; Schmid, W. E.; Trushin, S. A.; Fuss, W. *J. Phys. Chem. A* **2001**, *105*, 4458–4469.
- (11) Schonborn, J. B.; Sielk, J.; Hartke, B. *J. Phys. Chem. A* **2010**, *114*, 4036–4044.
- (12) Tapavicza, E.; Meyer, A. M.; Furche, F. *Phys. Chem. Chem. Phys.* **2011**, *13*, 20986–20998.
- (13) Geppert, D.; Seyfarth, L.; de Vivie-Riedle, R. *Appl. Phys. B: Laser Opt.* **2004**, *79*, 987–992.
- (14) Hofmann, A.; de Vivie-Riedle, R. *J. Chem. Phys.* **2000**, *112*, 5054–5059.
- (15) Anderson, N. A.; Sension, R. J. In *Liquid Dynamics: Experiment, Simulation, and Theory*; Fourkas, J. T., Ed.; American Chemical Society: Washington, DC, 2002; Vol. 820, pp 148–158.
- (16) Anderson, N. A.; Shiang, J. J.; Sension, R. *J. J. Phys. Chem. A* **1999**, *103*, 10730–10736.
- (17) Fuss, W.; Höfer, T.; Hering, P.; Kompa, K. L.; Lochbrunner, S.; Schikarski, T.; Schmid, W. E. *J. Phys. Chem.* **1996**, *100*, 921–927.
- (18) Tang, K.-C.; Rury, A.; Orozco, M. B.; Egendorf, J.; Spears, K. G.; Sension, R. *J. J. Chem. Phys.* **2011**, *134*, 104503.
- (19) Marzec, K. M.; Reva, I.; Fausto, R.; Malek, K.; Proniewicz, L. M. *J. Phys. Chem. A* **2010**, *114*, 5526–5536.
- (20) Frisch, M. J.; Trucks, G. W.; Schlegel, H. B.; Scuseria, G. E.; Robb, M. A.; Cheeseman, J. R.; Montgomery, J. A.; Vreven, T.; Kudin, K. N.; Burant, J. C. et al. *Gaussian 03*, revision C.02; Gaussian, Inc.: Wallingford, CT, 2004.
- (21) Peng, C. Y.; Schlegel, H. B. *Isr. J. Chem.* **1993**, *33*, 449–454.
- (22) Saltiel, J.; Waller, A. S.; Sears, D. F.; Garrett, C. Z. *J. Phys. Chem.* **1993**, *97*, 2516–2522.
- (23) Saltiel, J.; Sun, Y. P. *J. Phys. Chem.* **1989**, *93*, 6246–6250.
- (24) Strickler, S. J.; Berg, R. A. *J. Chem. Phys.* **1962**, *37*, 814–822.
- (25) Viscosity of Liquids. In *CRC Handbook of Chemistry and Physics*, 91st ed. (Internet Version 2011); Haynes, W. M., Ed.; CRC Press/Taylor and Francis: Boca Raton, FL, 2011.
- (26) The PyMOL Molecular Graphics System, Version 1.2r3pre, Schrödinger, LLC.
- (27) Trulson, M. O.; Dollinger, G. D.; Mathies, R. A. *J. Chem. Phys.* **1989**, *90*, 4274–4281.
- (28) Tang, K. C.; Sension, R. *J. Faraday Discuss.* **2011**, *153*, 117–129.
- (29) Meyer-Ilse, J.; Akimov, D.; Dietzek, B. *J. Phys. Chem. Lett.* **2012**, *3*, 182–185.